SCK•CEN
0096039

SCK•CEN

STUDIECENTRUM VOOR KERNENERGIE
CENTRE D'ÉTUDE DE L'ÉNERGIE NUCLÉAIRE

Unclassified

Constraint Assessment in Miniature C(T) Specimens using 3-D Finite Element Simulations

Convention Electrabel-SCK•CEN

M. Scibetta

RMR
SCK•CEN, Mol, Belgium

BLG-923

September 2002

DISTRIBUTION LIST

Author	SCK•CEN	1 copy
A. Al Mazouzi	SCK•CEN	1 copy
R. Chaouadi	SCK•CEN	1 copy
E. Lucon	SCK•CEN	1 copy
L. Malerba	SCK•CEN	1 copy
J.-L. Puzzolante	SCK•CEN	1 copy
J. Schuurmans	SCK•CEN	1 copy
E. van Walle	SCK•CEN	1 copy
R. Gérard	Tractebel	3 copies
Secretary RMO	SCK•CEN	5 copies
		Total of 16 copies

This document has been written and approved by:

		Date	Approval
Author:	M. Scibetta	26/8/2002	M Scibetta
Verified by:	E. Lucon	2/9/2002	[signature]
	J. Schuurmans	26/8/2002	[signature]
Approved by:	E. van Walle	3/9/02	[signature]

Unclassified

Constraint Assessment in Miniature C(T) Specimens using 3-D Finite Element Simulations

Convention Electrabel-SCK•CEN

M. Scibetta

BLG-923

Contractnr: KNT 90 99 1165.01

RMR
SCK•CEN, Mol, Belgium

September 2002

TABLE OF CONTENTS

ABSTRACT

The objective of this work is to compare the constraint of SE(B) and C(T) specimens having the same ligament size. This study is a support for the use of miniature C(T) specimen and to better understand the difference observed between standard C(T) and PCCv.

Another field of application is the correction of constraint for existing data sets that contain few or any valid data.

It is found that miniature C(T) specimens are subject to a loss of constraint which is similar to PCCv specimens.

KEYWORDS

Finite element calculations, three-dimension, PCCv, C(T), loss of constraint, fracture toughness

1 Introduction

Fracture toughness testing in the transition regime was recently standardised within the ASTM E1921-02 [1]. This standard proposes a procedure to analyse the test results of standard specimens and to determine the reference temperature, T_0, for ferritic steels in the transition range.

The embrittlement of Reactor Pressure Vessel Steels (RPVS) could be usefully assessed through the shift of the reference temperature ΔT_0 instead of the current semi-empirical methodology. In practice, standard one inch thick Compact Tension, 1T–C(T), specimens can be replaced with smaller fracture toughness specimens, such as the precracked Charpy V-notch (PCCv) or miniature C(T) specimen. Indeed, irradiated RPVS are available in small quantities and PCCv specimens and miniature C(T) can be reconstituted and/or machined from broken surveillance Charpy specimens [2, 8].

The published literature shows that the PCCv specimen analysed using the ASTM E1921-02 standard generally shows a 5 to 15 °C lower reference temperature than the C(T) specimen. Compared with the inherent scatter in the transition, this difference is small. However, it has been systematically observed on many materials [3]: JSPS [4, 5], 22NiMoCr37 [5], JRQ [5, 6], 73W [5], KFY5 [6] and JFL[6]. The reason for this difference was investigated in a previous report [7]. It was found that constraint loss is a plausible explanation for this difference.

However little information is available on miniature C(T) specimens [8], which could also be subject to the same loss of constraint effect.

The formulation and the level of constraint can be investigated using finite element simulations. However, a simple 2-dimensional analysis of a PCCv specimen, assuming a plane strain behaviour, is not an adequate model to accurately describe the actual 3-dimensional geometry [9, 10].

In order to develop a possible loss of constraint correction factor for small C(T) and to gain confidence in the results presented in [7, 10], a study was performed at SCK•CEN. This work was performed within Task 1.1.3 of the ELECTRABEL -SCK•CEN Convention 2002.

In this report, the finite element calculation of a mini C(T) specimen loaded up to 100 MPa√m is performed and compared to former results obtained on 1T–C(T) and PCCv specimens.

2 FE model

To model actual material behaviour, the incremental theory of plasticity is used in combination with an isotropic strain-hardening model based on the Von Mises criterion with a uniaxial true stress versus true strain function described by a power law:

$$\frac{\sigma}{\sigma_{YS}} = \begin{cases} \dfrac{\varepsilon}{\varepsilon_{YS}} & if\ \sigma < \sigma_{YS} \\ \left(\dfrac{\varepsilon}{\varepsilon_{YS}}\right)^{n} & if\ \sigma \geq \sigma_{YS} \end{cases} \tag{1}$$

$$\text{with} \quad \varepsilon_{YS} = \sigma_{YS} / E \tag{2}$$

The actual true stress versus true strain behaviour of metallic materials can generally be fitted by a power law curve. Alternatively, the strain-hardening exponent can be obtained from the following equation (3), which can easily be solved with a non-linear iterative solver. This expression was derived in [11] by solving the instability point and converting true stress to engineering stress.

$$\frac{\sigma_{TS}}{\sigma_{YS}} = \frac{\left(\dfrac{n}{\varepsilon_{YS}}\right)^{n}}{\exp(n)} \tag{3}$$

This study is limited to one material, representative of most unirradiated RPVS. It has a hardening exponent n=0.1, a Young modulus E=207 GPa, a Poisson ratio ν=0.3 and a yield stress such that E/σ_{YS} =500.

As most of valid fracture toughness tests on PCCv and C(T) specimens do not show any ductile crack growth, the modelling of ductile crack growth by a complex node release technique is not necessary.

8-node isoparametric hexahedral elements without reduced Gauss integration are used.

Because of large geometry changes, the modified updated Lagrangian [12] procedure is used to account for large strains and displacements. To avoid large mesh deformation and overlapping at the crack tip, an initial blunted mesh is used. The initial crack tip radius is 10 μm. The dimension of the smallest element located at the crack tip is typically one third of the initial crack tip radius.

The specimen dimensions of the selected mini C(T) are: W=10 mm and B=5 mm. According to ASTM terminology, the mini C(T) investigated in this study is the 0.2T–C(T). As ASTM E1921-02 states that a_0 shall be 0.5W±0.05W, a/W=0.5 is selected for the present study. To reduce computer time, only one fourth of the C(T) geometry was simulated (see Figure 1). Symmetry conditions were imposed to the planes defined by the equations y=0 and z=0. The machined notches for precracking and for clip gauge attachment are not modelled, as this will not affect the results. Only the non-side grooved geometry is investigated in this study.

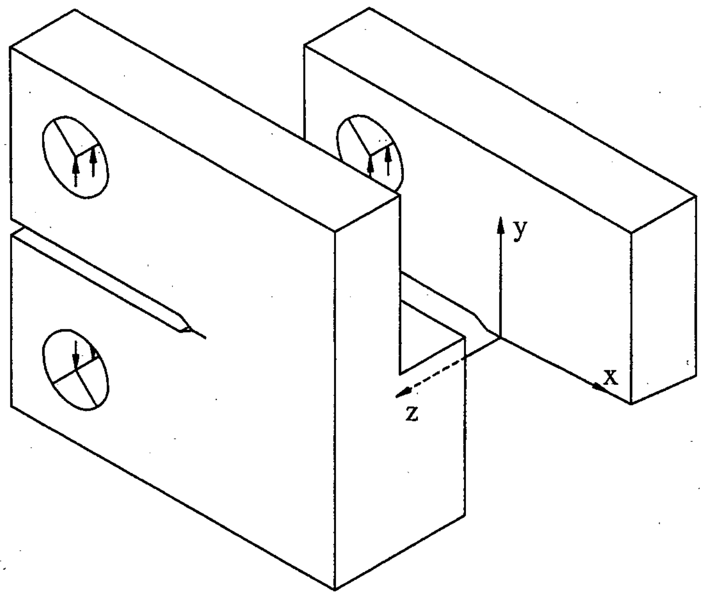

Figure 1 *C(T) specimen loaded in tension. Only one fourth of the geometry is simulated.*

Load is applied through contact conditions between the specimen and the loading pin. The introduction of these conditions in a finite element model is rather complex and introduces additional highly non-linear equations.

To simplify the problem, the contact is simulated by fixing the displacement in the $\vec{Y}$ direction on the nodes located in the centre of the hole. Elastic pentahedrons with the same Young modulus and Poisson ratio as the specimens are used to improve the load distribution on the contact areas (see Figure 1).

To model the geometry, it is simple to use a regular mesh, which is straightforward to generate. However, this would require a very long computer time for a given accuracy. The preferred strategy is to use a fine meshing in deformed regions and a coarse mesh in regions that are less deformed. The mesh density is selected according to the experience gained with finite element calculation of the PCCv specimen loaded in three point bending [13]. The mesh contains 5120 elements and 6184 nodes and is depicted in Figure 2.

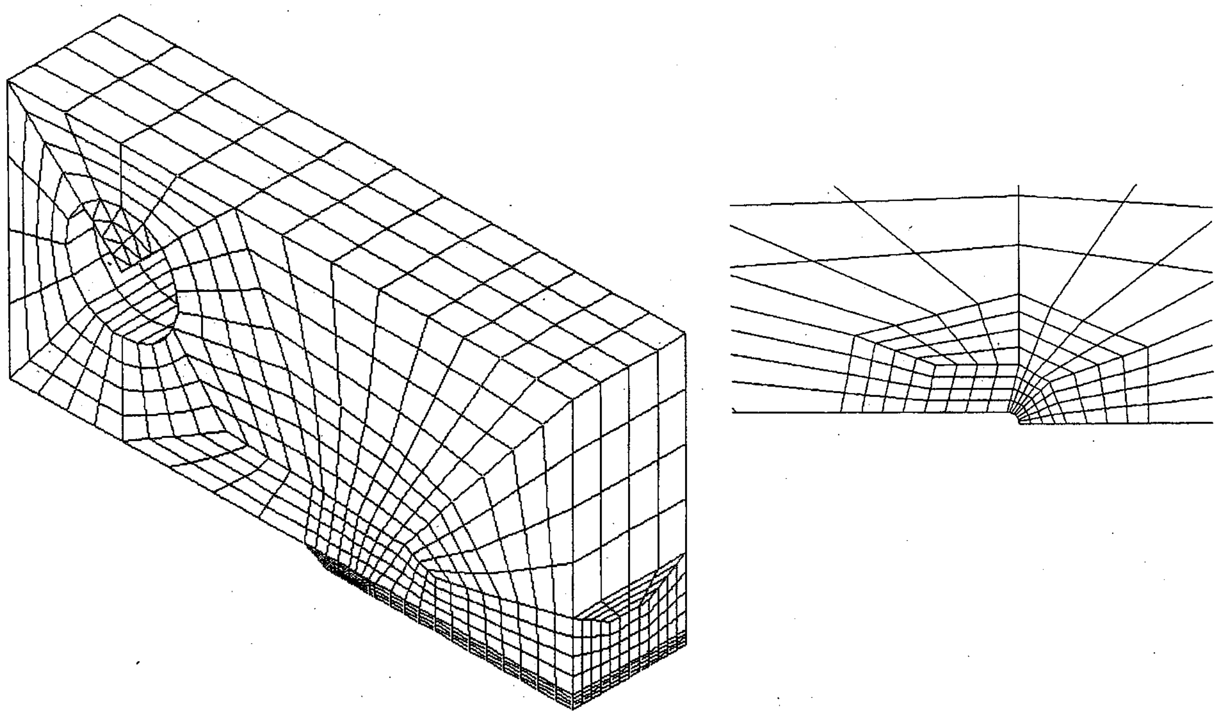

Figure 2 Meshing of a 0.2T−C(T) specimen without side-grooves.

The finite element code used, SYSWORLD, is a standard commercial code developed by the ESI group [12]. The algorithm for the matrix inversion uses an iterative method to reduce the size of the required memory. The resolution of non-linear equations is performed using the BFGS[1] algorithm. The number of load increments is typically 50.

The machine used for this project is a standard PC running under Windows XP. The central process unit (CPU) time per load increment is 186 sec. The total execution time is higher than the indicated CPU time because the management of the operating system and the pre- and post-processing time are not taken into account.

3 Finite element results

The load versus crack mouth opening displacement (CMOD) diagram is given in Figure 3. The initial crack mouth opening or gauge length is taken equal to 0.548 mm. The CMOD is equivalent to the load line displacement (LLD) for a C(T) specimen. Figure 3 shows a typical non-linear behaviour.

[1] Broyden, Fletcher, Goldfarb, and Shanno

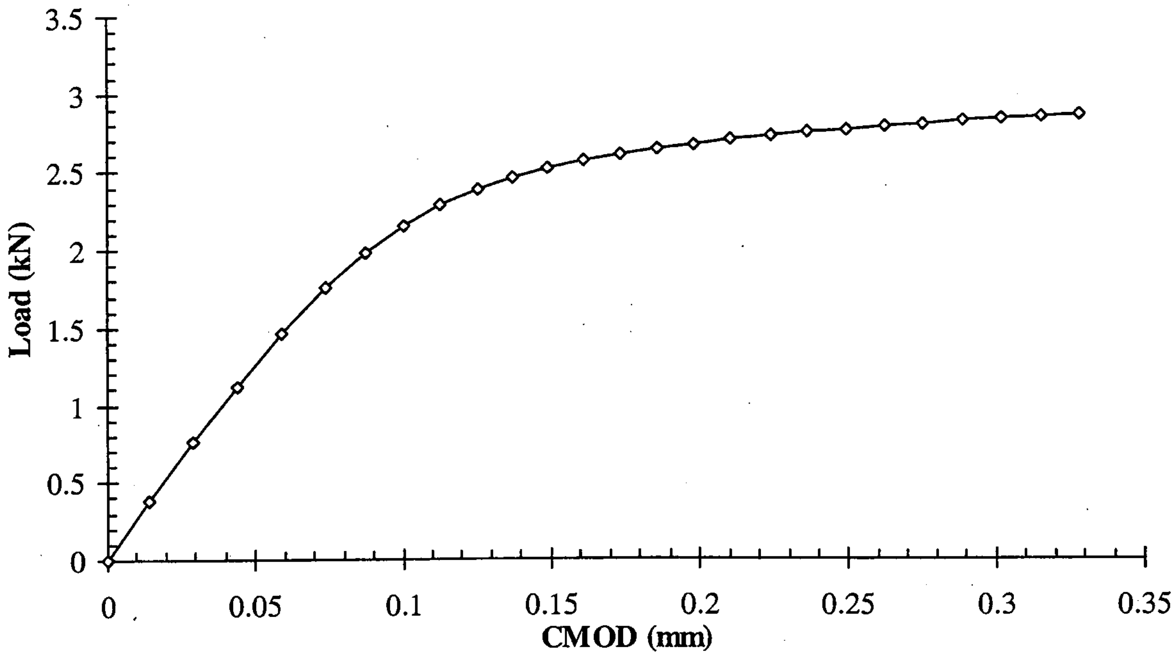

***Figure 3** Load versus CMOD (LLD) for a 0.2T–C(T) specimen loaded to 117MPa√m.*

The constraint of the 0.2T–C(T) specimen is now compared to the constraint of a 1T–C(T) specimen. When no loss of constraint correction is taken into account, the reference temperature for a 0.2T–C(T) specimen is obtained as:

$$T_{0,0.2T-C(T)} = T - \frac{1}{0.019}\ln\left(\frac{K_{med,1T} - 30}{70}\right) \quad (4)$$

where T is the test temperature, $K_{med,1T}$ is the median fracture scaled to one inch:

$$K_{med,1T} = 20 + (K_{med} - 20)\left(\frac{B}{B_{1T}}\right)^{1/4} \quad (5)$$

where K_{med} is the median fracture toughness of the 0.2T–C(T) specimens, B the original specimen thickness (according to the standard the net thickness B_N should not be used) and B_{1T} a reference length of one inch. In this case B=5mm and B_{1T}=25.4mm.

To take loss of constraint into account, a simple model proposed by Anderson and Dodds [14] and developed in [11] is used. The reference temperature is obtained using:

$$T_{0,0.2T-C(T)} = T - \frac{1}{0.019}\ln\left(\frac{K_{med,1T,0.2T-C(T)} - 30}{70}\right) \quad (6)$$

where $K_{med,1T,0.2T-C(T)}$ is the median fracture of the 0.2T–C(T) specimens corrected for size and loss of constraint to an equivalent 1T–C(T) specimen:

$$K_{med,1T,0.2T-C(T)} = 20 + (K_{med} - 20)\left(\frac{A_{0.2T\text{-}C(T)}}{A_{C(T)}}\frac{B}{B_{1T}}\right)^{1/4} \tag{7}$$

with

$$A = \frac{\sigma_{YS}^2 \varepsilon_{YS}^2}{B\,J^2} V(\sigma_1) \tag{8}$$

where $V(\sigma_1)$ is the volume over which the maximum principal stress is equal or greater than a certain value σ_1.

The dimensionless area, A, is given in Figure 4 as a function of the principal stress. This dimensionless area is obtained by finite element calculations on five different configurations, SSY plane strain, SSY plane stress, PCCv, 1T–C(T) and 0.2T–C(T). SSY refers to the Small Scale Yielding solution, which is a 2D solution of a small plastic zone embedded in a large elastic zone [11].

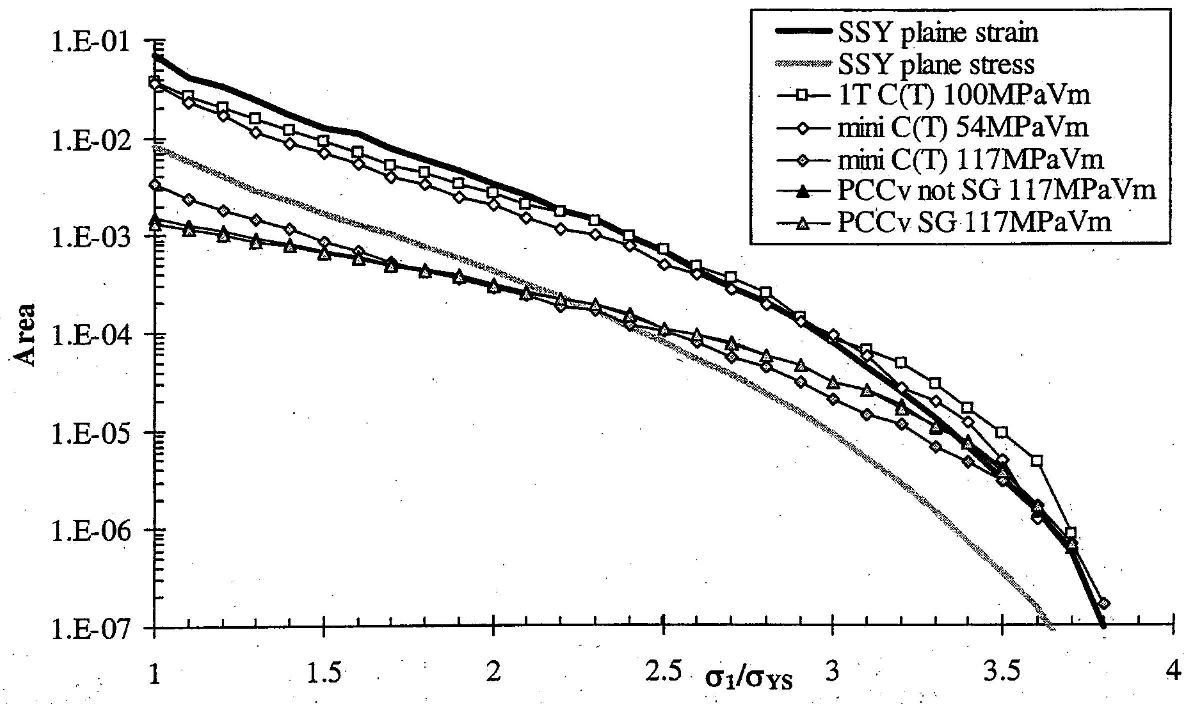

Figure 4 Dimensionless area, A, for which the maximum principal stress is above a given value σ_1.

It is now possible to evaluate the loss of constraint through:

$$\Delta T = T_{0,\text{mini } C(T)} - T_{0,C(T)} \tag{9}$$

ΔT is given in Figure 5 as a function of K_{med} and σ_1. The geometry studied is the non-side grooved 0.2T–C(T) and the reference solution is the non-side grooved 1T–C(T) geometry.

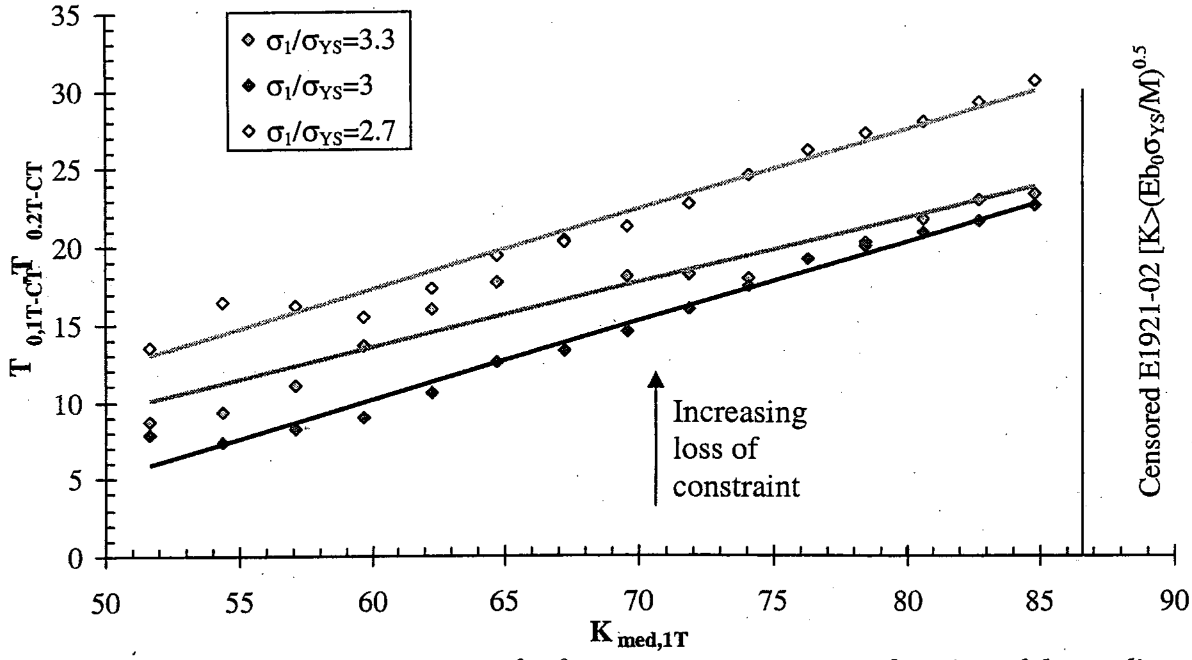

***Figure 5** Loss of constraint in terms of reference temperature as a function of the median fracture toughness normalised to 1T and for different critical stresses.*

4 Discussion

The constraint of a 0.2T–C(T) geometry can be discussed based on Figure 4. Up to 54 MPa√m, no constraint difference is observed between 1T–C(T) and 0.2T–C(T). It is clear that at a relatively low load, 1T–C(T) and 0.2T–C(T) specimens are closer to plane strain than to plane stress. As already found in [7], the constraint just ahead of the crack tip at σ_l/σ_{YS}=3.5 is even higher than the plane strain SSY solution.

Figure 4 clearly shows a loss of constraint in function of the loading level for the 0.2T–C(T) and PCCv geometry. This loss of constraint is strongly dependent on the maximum principal stress considered or equivalently to the considered distance. Consequently, the scaling results, illustrated in Figure 5, depend on the maximum principal stress level considered. This means that a better description of the failure mechanism such as the BEREMIN model [15], would be required to further determine the effect of loss of constraint. In a recent work, Ruggieri et al. [16] demonstrated the non-uniqueness of the (m, σ_u) parameters of the BEREMIN model. They found a strong sensitivity of corrected J_c-value on parameter m. This means that the constraint correction is a function of the failure mechanism. It should be noted that for the Cracked Round Bar, (CRB), geometry, the loss of constraint correction was found to be nearly independent of the maximum stress considered [11]. Taking a plausible stress contour of 3 times σ_{YS}, it is found that 0.2T–C(T) specimens tested at the same temperature as 1T–C(T) specimens should lead to about 10 to 15 °C lower reference temperatures.

The constraint of the PCCv and the 0.2T–C(T) loaded to 117MPa√m is practically equivalent. Therefore, it is expected that 0.2T–C(T) will lead to the same reference temperature bias than PCCv. Up to now only very limited experimental data is generated on the 0.2T–C(T) specimen. However, the data available in [8] support that a bias exist for 0.2T–C(T).

CONCLUSIONS

Three-dimensional finite element calculations were performed on non side-grooved mini C(T) specimens for a/W=0.5, B=5 mm and W=10 mm. The loss of constraint assessment is addressed in this report.

The main outcomes of this investigation are:

- 1T–C(T), 0.2T–C(T) and PCCv specimens display a plane strain behaviour at low load levels.
- For load levels up to 54 MPa√m practically no constraint difference between 0.2T–C(T) and 1T–C(T) is observed.
- For a 0.2T–C(T) loaded above 54 MPa√m, which correspond to $M_{C(T)}$=146, the constraint decreases as compared with 1T–C(T).
- The model used predicts a reference temperature about 10 to 15 °C lower for a 0.2T–C(T) specimen as compared to a 1T–C(T) specimen. The limited experimental data found in the literature support this important result. However, it is recommended to perform additional experimental work on the miniature C(T) specimen.

ACKNOWLEDGEMENTS

The present work is partly financed by Electrabel. Their support is kindly appreciated.

REFERENCES

[1] ASTM E 1921-02 "Test method for the determination of reference temperature, T_0, for ferritic steels in the transition range", 2002

[2] E. van Walle "Reconstitution: where do we stand ?", Effects of irradiation on materials: 17th international symposium, ASTM STP 1270, D.S. Gelles, R.K. Nansdstad, A.S. Kumar and E.A. Little, Eds., American Society for Testing Materials, 415-441, 1996

[3] K. Wallin "Applicability of miniature size bend specimens to determine the master curve T_0 Temperature", IGRDM-9, Leuven, Belgium, September 2000

[4] E. Lucon and M. Scibetta "Comparison between precracked Charpy-V and C(T) specimens for T_0 determination of the JSPS RPV steel", report R-3378 Rev. 1, SCK•CEN, Mol, Belgium, January 2000

[5] R. Chaouadi, M. Scibetta, E. van Walle and R. Gerard "On the use of the master curve based on the precracked charpy specimen", Pressure Vessel and Piping Symposium, "Fracture, Fatigue and Weld Residual Stress ", Vol 393, pp. 35 -46, 1999

[6] Lee Bong-Sang, Yang Won-Jon, Kim Joo-Hag, Hong Jun-Hwa and Lee Byong-Whi "Determination of the fracture toughness transition temperature, T_0, of the IAEA and Korean Reference Materials, JRQ, JFL, KFY5", presented at the RCM of the CRP on "Assuring Structural Integrity of Reactor Pressure Vessels", Vienna Austria, November 17-19, 1999

[7] M. Scibetta "Constraint Assessment in PCCv and 1T C(T) Specimens using 3-D Finite Element Simulations" Convention Electrabel-SCK•CEN, Report BLG-861, SCK•CEN, Mol, Belgium, 2000

[8] M. Scibetta "Optimum Use of Broken Charpy Specimens from Surveillance Programs for the Application of the Master Curve Approach" to be published in International Journal of Fracture

[9] Dodds R.H., Carpenter W.C. and Sorem W.A. "Numerical evaluation of a 3-D J-integral and comparison with experimental results for a 3-point bend specimen", Engineering Fracture Mechanics Vol. 29, No. 3, pp. 275-285, 1988

[10] Nevalainen M. and Dodds R.H.Jr. "Numerical investigation of 3-D Constraint Effects on Brittle Fracture in SE(B) and C(T) Specimens", Report UILU-ENG-95-2001, Department of civil engineering, university of illinois at Urbana-Champaign Urbana, Illinois, February 1995

[11] Scibetta M. "Contribution to the Evaluation of the Circumferentially-Cracked Round Bar for Fracture Toughness Determination of Reactor Pressure Vessel Steels", Dissertation for the Degree of Doctor in Applied Sciences, Université de Liège, March 1999.

[12] ESI Group, SYSTUS+ 2.0, Analysis Reference Manual, 1998

[13] M. Scibetta "3-D Finite Element Simulation of the PCCv Specimen Statically Loaded in Three-Point Bending" Convention Electrabel-SCK•CEN, Report BLG-960 Revision 1, SCK•CEN, Mol, Belgium, 2001

[14] Anderson T.L. and Dodds R.H. Jr. "Simple constraint corrections for subsize fracture toughness specimens", Small Specimen Test Techniques Applied to Nuclear Reactor Vessel Thermal Annealing and Plant Life Extension, ASTM STP 1204, Corwin W.R., Haggag F.M. and Server W.L., Eds., American Society for Testing and Materials, Philadelphia, pp. 93-105, 1993

[15] Beremin F.M. "A local criterion for cleavage fracture of a nuclear pressure vessel steel", Metallical transactions A, Vol. 14A, pp. 2277-2287, 1987

[16] Ruggieri C., Gao X., Dodds R.H.Jr. "Transferability of the elastic-plastic fracture toughness using the Weibull stress approach: significance of parameter calibration", Engineering Fracture Mechanics 67, pp. 101-117, 2000